



Improvement of metakaolin on radioactive Sr and Cs immobilization of alkali-activated slag matrix

Qian Guangren*, Li Yuxiang, Yi Facheng, Shi Rongming

School of Materials Science and Engineering, Southwest University of Science and Technology, Mianyang 621002, Sichuan, PR China

Received 26 June 2001; received in revised form 10 January 2002; accepted 24 January 2002

Abstract

Effects of metakaolin on simulated radioactive Sr or Cs immobilizing behavior of alkali-activated slag (AAS) matrix were evaluated by cation exchange capacity (CEC), distribution ratio of selective adsorption, leaching test and porosity analyses. The results revealed that the additions of metakaolin into the AAS matrixes largely enhanced their distribution ratios K_d of selective adsorption on Sr and Cs ions. Meanwhile, this new immobilizing matrix M-AAS showed the lowest leaching rate. Hydration product analyzes by XRD, DTA, FTIR and SEM demonstrated that (Na + Al)-substituted calcium silicate hydrate (CSH) and self-generated zeolite were major hydration products in the M-AAS matrix. These products have better Sr and Cs selective adsorption as compared to C-S-H without any substitution and natural zeolite minerals. © 2002 Elsevier Science B.V. All rights reserved.

Keywords: Metakaolin; Alkali-activated slag; Selective adsorption; Simulated radioactive Sr or Cs waste; Hydration products

1. Introduction

Immobilization and solidification of hazardous cations like ^{137}Cs and ^{90}Sr is one of the important keys in handling the radioactive wastes of nuclear power plants. Portland cement has been the most common matrix for immobilizing this kind of radioactive waste. Calcium silicate hydrate (CSH) is a major hydrate product, responsible for the strength development of cement paste. This hydration product has a layer structure similar to those of 2:1 clay minerals. The cation exchange and selective adsorption ability of CSH product are intermediate between those of natural clay minerals and natural zeolites [1]. Moreover, CSH product is thermodynamically stable in Portland cement environment whereas zeolites

* Corresponding author. Present address: Environmental Engineering Research Center, School of Civil and Environmental Engineering, Nanyang Technological University, Singapore 639798, Singapore. Fax: +65-8615254. E-mail address: cgrqian@ntu.edu.sg (Q. Guangren).

and clays are not. It has been therefore recognized as a new family of cation exchangers for immobilization of radionuclides and heavy metals [2–4]. However, ordinary Portland cement matrix (OPC) has some disadvantages such as high porosity and poor durability in practical application. Additionally, the pore solution of paste is always saturated with calcium hydroxide during the hydration of Portland cement, so that radioactive nuclides caesium and strontium still cannot be well immobilized in the matrix of CaO-rich CSH [5,6].

Compared to CSH, zeolite minerals are a framework silicate with rigid and very open cavity, which have the best selectivity for radionuclides among various cation exchanges. As cation exchanges and adsorbents, natural zeolite minerals have been extensively introduced into the OPC matrix for removing radioactive cations [7,8].

Alkali-activated slag (AAS) binder is a non-traditional cementitious material that relies on the alkali activation of aluminosilicate materials, which is made from 100% slag plus activator. When this AAS matrix is used as barriers or for encapsulation, it can not only effectively reduce the permeability of the matrix but fix nuclide ions in the structure with large cage-like crystals [9,10]. This excellent effect is attributed to the formation of two thermodynamical stable phases such as CaO-low CSH [11,12] and self-generated zeolitic phase [13].

The CSH formed in both the OPC matrix and AAS matrix is nearly unsubstituted. It has been realized that (Al+Na)-substituted CSH exhibits much better cation exchange capacity (CEC) and selective adsorption for Cs ion than unsubstituted CSH [14,15]. For example, kaolinite–OPC mixture can effectively fix radioactive ^{137}Cs [16].

Metakaolin is a highly reactive metastable clay mineral. The alkali activation of metakaolin has appeared excellent potential in making new chemically bonded cementitious materials, in which metakaolin as a source of reactive aluminium can induce the formation of zeolitic product [17,18].

In order to form the hydration products such as (Al + Na)-substituted CSH and self-generated zeolite, the author developed a new aluminium-rich AAS matrix (M-AAS) by adding metakaolin and other clay adsorbents into the AAS matrix. This new immobilizing matrix has been proved to have much better immobilizing effect on Sr and Cs ions.

This paper is to report the effect of metakaolin addition on the immobilizing behavior of AAS matrix such as Cs or Sr selective adsorption, leachability and hydration products.

2. Experiments

2.1. Raw materials

Blast furnace slag (BFS) was used as the main raw material to synthesize an AAS matrix. The chemical compositions of this slag are shown in Table 1. The surface area of the slag was $520\text{ m}^2/\text{kg}$.

After evaluating the selective adsorption and CEC of different clays, the three clays with optimal selective adsorption, i.e. metakaolin, NaOH-treated attapulgite clay and natural zeolite, were selected for the adsorbents of AAS matrix. Meanwhile, metakaolin clay was used as a source of active aluminium in order to induce the formation of zeolitic products.

Table 1
Chemical compositions of main raw materials (wt.%)

	CaO	SiO ₂	Al ₂ O ₃	Fe ₂ O ₃	MgO	TiO ₂	Na ₂ O
BF slag	46.74	36.27	9.71	0.86	5.52	2.80	
Metakaolin	0.22	53.47	44.79	0.06	0.05	0.05	
Water glass		30.4					13.1

Table 1 lists the chemical compositions of metakaolin. It was produced from the decomposition of natural kaolinite clay burned at 650 °C for 2 h and then ground into powder of 380 m²/kg.

2.2. (Al + Na)-substituted CSH and NaA-zeolite

Three (Al+Na)-substituted CSH phases with different constituents, 0, 5, 10 mol% Al₂O₃ for SiO₂ and Na₂O/Al₂O₃ kept 0.5 mol%, were hydrothermally synthesized. The ideal chemical formula of unsubstituted CSH is Ca₅Si₆(OH)₂·2H₂O (CaO/SiO₂ = 0.8). CaO, metakaolin and NaOH were used as raw materials. CaO was made by heating reagent grade CaCO₃ for 4 h at 1100 °C. The molar ratio of CaO/(SiO₂ + Al₂O₃) was maintained at 0.8 by adding amorphous SiO₂ gel. The samples were first mixed uniformly into slurry with distilled water and then treated at 140 °C for 8 h. After hydrothermal treatment, the solid and solution were separated and dried in the vacuum.

NaA-zeolite with formula 0.99Na₂OAl₂O₃1.95SiO₂·4H₂O was synthesized at 50 °C. Metakaolin powder was placed into 2 M NaOH solution at a water/solid ratio of 2.5. The sample was firstly stirred for 5 h and then kept in sealed plastic bottles for 7 days at 50 °C.

2.3. Preparation of immobilizing matrixes

Six immobilizing matrixes were made from different raw materials as listed in Table 2. The cement pastes containing 0.5 wt.% Cs⁺ (CsCl) or Sr²⁺ (SrCl₂·6H₂O) were cast in a cylindrical mould, with a diameter of 2.5 cm and a height of 5 cm and cured in a fog room at 25 °C for 28 days. Ratio of water to solid in the pastes was 0.3. The alkali activators were

Table 2
Distribution ratio K_d of selective adsorption for different immobilizing matrixes

Samples	Proportion (wt.%)				Distribution ratio K_d (ml/g)	
	OPC	Slag	MK	Clay adsorbents	Cs	Sr
OPC	100				1537	4651
AAS		100			3860	6403
AAS1	95		5		4226	7054
AAS2	90		10		5103	7793
AAS3	85		15		6043	8971
M-AAS		70	10	20	6447	12050

Note: MK: metakaolin; OPC: ordinary Portland cement.

water glass and sodium carbonate. The addition of alkali activator was adjusted to 5% (by Na_2O) of slag in weight.

2.4. Determination of cation exchange and selective adsorption capacity

Cation exchange capacities for synthesized (Al + Na)-substituted CSH and NaA-zeolite were measured by using a method as described by Komarneni and Roy [7]. Briefly, the method is as follows. A known weight of the sample was equilibrated with 1 N KCl solution followed by five washings with 0.01 N KCl to remove the excess of KCl and to prevent hydrolysis. The K^+ was then displaced by Cs on repeated washings with 1 N CsCl. The displaced K^+ was determined by WYX-403 atomic emission spectroscopy (made in China).

Cs or Sr selective adsorption by various minerals and six immobilizing matrixes without Sr or Cs ion were determined by adding 25 ml 0.002 N CsCl or SrCl_2 solution to 50 mg of samples, equilibrating for 7 days in glass vials, separating the solid and solution phases by centrifugation and analyzing Cs or Sr ion in solution by atomic absorption spectroscopy.

2.5. Hydration products, porosity and leachability analyses

After six immobilizing matrixes were cured for 28 days, one part of each specimen was employed for hydration product analyses by D/max-III X-ray diffractometer (XRD), TAS-100 thermoanalyzer (DTA-TG), JSM-5410 scanning electron microscopy (SEM), Perkin Elmer fourier transform infrared spectrometer (FTIR) and porosity analysis by Quantachrome scanning mercury porosimeter. The leach rates of immobilizing matrixes were determined according to GB7023-86 (a P.R.C. standard method). The method is to place the specimen into deionized water solution in a Teflon container at 25 °C for different time durations. The volume of solution was 100 ml. The cylinder used for the leach tests was 5 cm in height and 2.5 cm in diameter. The concentration of Sr or Cs ion in the leachate was analyzed by atomic adsorption spectroscopy.

3. Results and discussion

3.1. Sr or Cs adsorption and leachability of immobilizing matrix

3.1.1. Distribution ratio K_d

The effects of metakaolin on Sr or Cs ion selective adsorption of AAS matrix were evaluated by the distribution ratio K_d [15]. The distribution ratio K_d is defined as the ratio of the amounts of ions adsorbed by a unit mass of solid adsorbent to the equilibrium concentration of ion in the aqueous phase. Table 2 shows the results of distribution ratio K_d of different matrixes. Traditional OPC matrix was made from ordinary Portland cement. It had the lowest distribution ratio K_d , 4651 ml/g for Sr ion and 1537 ml/g for Cs ion. The distribution ratio K_d of AAS matrix was highly advanced and it increased to 6403 ml/g for Sr ion and 3860 ml/g for Cs ion, 38–151% higher than those of OPC matrix, respectively. This indicates that the improvement of AAS matrix on selective adsorption behavior for

Cs ion was much more effective than for Sr ion. Additions of metakaolin into AAS matrix had a positive effect to further enhance their selective adsorption on Sr and Cs ions, which was supported by the fact that the distribution ratio K_d increased with metakaolin additions. AAS3 matrix contained 15% metakaolin and its distribution ratio K_d was 8971 ml/g for Sr ion and 6043 ml/g for Cs ion, 40–56% larger than those of AAS matrix without metakaolin. As a result, the new immobilizing matrix M-AAS, in which metakaolin and other clay adsorbents were added into AAS matrix, exhibited the highest Sr and Cs distribution ratios K_d among six matrixes, i.e. 12 050 ml/g for Sr ion and 6447 ml/g for Cs ion, which was 1.5–3.1 times larger than those of OPC matrix and 67–88% higher than those of AAS matrix.

3.1.2. Leachability

The leachability of matrix is an important index to evaluate the adsorption behavior and immobilizing effect. The leachability of three matrixes containing 0.5 wt.% Sr^{2+} or Cs^+ was expressed by the leaching rate R (cm per day) as the Eq. (1). The leaching rate R has the dimension of speed.

$$R_n^i = \frac{a_n^i / A_0^i}{(F/V)t_n} \quad (1)$$

where i is the Sr^{2+} or Cs^+ ion; a_n the mass of leached Sr^{2+} or Cs^+ ion at certain period (g); A_0 the mass of initial addition for Sr^{2+} or Cs^+ ion in the specimen (g); F the surface area of the specimens (cm^2); V the volume of the specimen (cm^3) and t_n the leaching time.

Table 3 lists the leaching rates of three immobilizing matrixes with simulated radioactive nuclide Sr or Cs ion at 25 °C. The leaching rate of three matrixes for Sr or Cs ion decreased in the order $\text{OPC} > \text{AAS} > \text{M-AAS}$, that is to say, M-AAS matrix exhibited the lowest leaching rate while OPC was the highest at any time. These results were well in line with the distribution ratios K_d of these matrixes. The higher the distribution ratio K_d , the less the leachability was. Theoretically, the leachability of matrix also depends on the porosity and the distribution of pore size in the matrix besides selective adsorption. The pore structure characteristics of three matrixes are summarized in Table 4. OPC matrix had the largest porosity 20.41% among three matrixes and its porosity consisted of 53% medium pores

Table 3
Leaching rate of simulated radioactive Sr or Cs ion in different immobilizing matrixes

Samples		Leaching rate R_n^i (10^{-6} cm per day)									
		1 Day	3 Days	7 Days	10 Days	14 Days	21 Days	28 Days	35 Days	42 Days	
M-AAS	Sr^{2+}	0.59	0.12	0.06	0.03	0.02	0.01	Trace	Trace	Trace	
	Cs^+	1.56	0.53	0.25	0.12	0.07	0.03	0.02	0.015	Trace	
AAS	Sr^{2+}	0.65	0.15	0.08	0.04	0.02	0.01	Trace	Trace	Trace	
	Cs^+	2.13	0.84	0.56	0.29	0.17	0.10	0.05	0.04	0.03	
OPC	Sr^{2+}	2.83	1.02	0.60	0.20	0.09	0.05	0.04	0.02	0.01	
	Cs^+	4.40	2.32	0.92	0.45	0.29	0.17	0.12	0.06	0.04	

Table 4
Porosity and pore size distribution of immobilizing matrixes

Sample	Pore size distribution V_p (% , nm)							Porosity (%)
	<4.6	4.6–9.2	9.2–18.3	18.3–36.6	36.6–73.2	73.2–146.5	>146.5	
M-AAS	16.37	65.46	8.38	2.68	1.84	1.36	3.91	17.87
AAS	15.84	73.90	5.00	2.41	2.00	0.18	0.69	11.63
OPC	9.86	25.87	46.22	3.79	1.90	1.23	11.13	20.41

(10–100 nm) and 11% large pores (>100 nm). M-AAS matrix and AAS matrix possessed similar pore structures. Their pore size distributions were concentrated on small pores (<10 nm), which represented over 80% of the porosity. The quantities of medium pore and large pore in the M-AAS matrix were slightly larger than those in the AAS matrix. This result seemed to contradict the lowest leachability of M-AAS matrix. The results thereafter would establish that the adsorption behavior of matrix is much more important than the pore structure.

3.2. The hydration products of immobilizing matrix

The excellent adsorption behavior of M-AAS matrix with metakaolin and clay adsorbents was well corrected with its hydration products. The hydration products were identified by XRD, DTA-TG, FTIR and SEM.

3.2.1. XRD

Fig. 1 shows the XRD results of original slag and immobilizing matrixes. There existed a broad and diffuse hump around $30\text{--}31^\circ$ (2θ), which arises from the original slag reflecting the short-range order of slag glass structure. After being alkali-activated for 28 days, a new peak superimposed on the amorphous hump, at 3.03 \AA , can be identified in the samples AAS and M-AAS. It can be attributed to the (1 1 0) reflection of poor crystalline CSH [19].

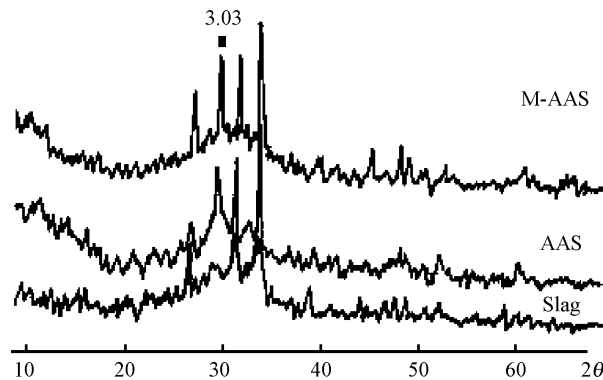


Fig. 1. XRD patterns of slag and immobilizing matrixes.

Although Glukhovskiy [13] found in 1959 that zeolite is a major hydration product formed in the AAS matrix, it has not been verified by later researches. However, it has been accepted that the addition of aluminium-rich materials such as metakaolin and fly ash into AAS would accelerate the formation of zeolitic products, which was confirmed by NMR [20]. For the sample M-AAS added with metakaolin, no trace of newly formed zeolite was found in XRD pattern, as the zeolitic products formed under normal ambient are amorphous [21].

3.2.2. DTA

The CSH phase gave a steeper endothermic peak with bigger weight loss at 130 °C and a broad exothermic peak at 800–900 °C in DTA curve (Fig. 2), which correspond to the gradual dehydration of the CSH interlayer and the decomposition of CSH into wollastonite. The exothermic peak of AAS matrix stood at 810 °C while that of M-AAS matrix was shifted to a higher temperature lying at 860 °C. M-AAS matrix was added with metakaolin,

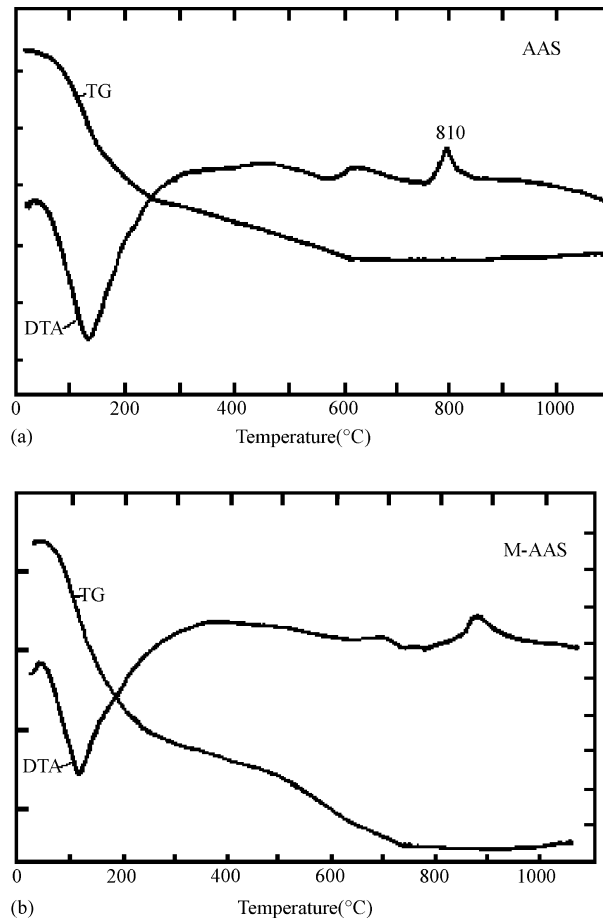


Fig. 2. DTA & TG curves of immobilizing matrixes. (a) AAS matrix; (b) M-AAS matrix.

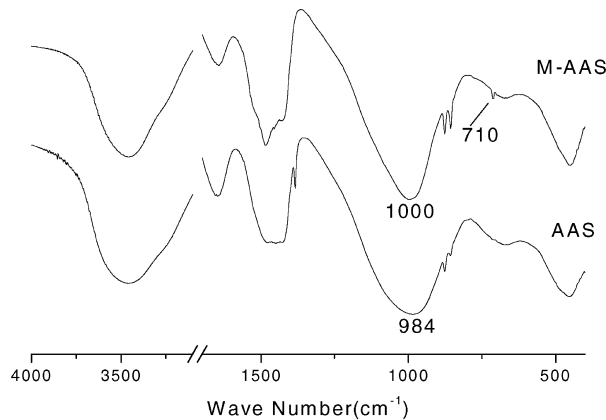


Fig. 3. Infrared absorption spectra of immobilizing matrixes.

belonging to Al_2O_3 -rich $\text{NaO-Al}_2\text{O}_3\text{-SiO}_2\text{-CaO-H}_2\text{O}$ system. Diamond and others [22,23] proved that the position shift of exothermal peak in DTA was due to the corporation of Al^{3+} into CSH to replace Si^{4+} . The non-equilibrium charge is compensated with an alkali ion such as Na^+ . It confirms that CSH in the M-AAS matrix is (Na + Al)-substituted CSH.

In addition, a poor endothermic peak at 750°C and small weight loss can be detected in DTA curve (Fig. 2b), which was absent from the AAS matrix (Fig. 2a). This endothermic peak is matched with that of phillipsite zeolite. This fact suggests that metakaolin addition favors the formation of self-generated zeolite.

3.2.3. FTIR

The FTIR results also proved the existence of hydration products such as (Na + Al)-substituted CSH and zeolitic phase in the M-AAS matrix. As shown in Fig. 3, there appeared two absorption bands at $3470\text{--}3450\text{ cm}^{-1}$ and $1655\text{--}1650\text{ cm}^{-1}$ in the AAS and M-AAS matrix, which are respectively due to the stretching and deformation vibrations of OH and H–O–H groups and from water molecules. There existed another strong absorption band at 984 cm^{-1} in the AAS matrix, which linked with the stretch vibration of Si–O of CSH [24]. But in the M-AAS matrix, this stretch vibration frequency was shifted to a higher position at 1000 cm^{-1} and a new weak absorption band at 710 cm^{-1} appeared. These bands were thought to be indicative of a zeolitic precursor [17]. Meanwhile, the shift of the stretch vibration from 984 cm^{-1} to 1000 cm^{-1} was also linked to the formation of new structure at which the SiO_4^{4-} groups were replaced by AlO_3^{4-} groups as network formers [25]. It further supported that CSH formed in the M-AAS matrix is (Na + Al)-substituted CSH.

3.2.4. SEM

The morphologies of hydration products in the M-AAS matrix were identified by SEM method. As shown in Fig. 4, (Al + Na)-substituted CSH was shorter fibre with a length

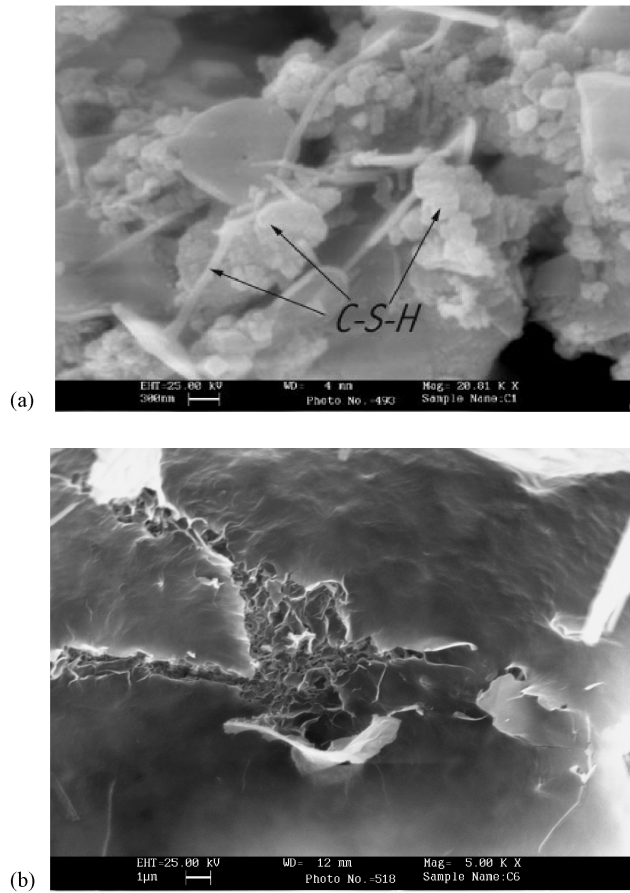


Fig. 4. SEM morphology of hydration products in the M-AAS matrix. (a) (Al + Na)-substituted CSH; (b) self-generated zeolite.

of 1 μ and thin cotton wool-like with a width of only several nanometers. Self-generated zeolite products appeared flakes-like ripples. Their sizes were only less than several microns in length. It indicates that all the hydration products in the M-AAS matrix were amorphous.

Based on above identified results, the major hydration products of M-AAS matrix were considered to be (Al + Na)-substituted CSH and self-generated zeolite precursor. In fact, zeolite phase formed in the AAS matrix is non-crystalline and therefore very difficult to characterize structurally with recently ordinary analytical tools such as XRD, which was supported by Glasser's view [26] that zeolite phase in the metakaolin-added cement materials with activator is a gel phase. Roy [21] also considered that new methods are needed for characterizing the constituents and structures of AAS system. To get sound evidences of the presence of zeolite precursor in the M-AAS matrix, thus, more detail works are still needed.

3.3. Cation exchange capacity and distribution ratio K_d for (Al + Na)-substituted CSH and NaA-zeolite

To well understand the contribution of hydrate products (Al + Na)-substituted CSH and zeolite on Sr and Cs selective adsorption behavior of M-AAS matrix, (Al + Na)-substituted CSH and zeolite were synthesized and their CECs and distribution ratios K_d for Sr and Cs ions were evaluated.

To synthesize (Al + Na)-substituted CSH and zeolite products, metakaolin was selected for the main source of active aluminium and silica other than lime and amorphous silica gel. To obtain poorly crystallized CSH rather than well crystallized tobermorite, the treatment condition was maintained at 140 °C for 8 h. The zeolitic product synthesized by metakaolin source was NaA-zeolite [27].

Table 5 gives the CEC of different synthesized minerals. As is well known, there are three causes that control the CEC of minerals, broken bonds around the edges of the silica-alumina units, lattice substitution and the hydrogen of exposed hydroxyls [28]. Sample A00, CSH without any substitution, had a 32 meq/100 g of CEC. This CEC was higher than that of crystallized tobermorite, 12 meq/100 g [15]. It should be attributed to the fact that CSH contained much more broken bonds due to its poor crystallization than well crystallized tobermorite although they all do not get the contribution from lattice substitution. However, when Al^{3+} and Na^+ were incorporated into CSH, their CEC values were largely improved. It appeared 111–162 meq/100 g of CEC, 3–4 times higher than CSH without any substitution. Evidently, a lot of isomorphous substitutions of Al^{3+} for Si^{4+} in CSH should account for this in addition to much larger specific surface of amorphous products. Zeolitic group minerals have the so-called molecular sieve structures with channels other than lattice substitutions. Natural zeolite XJZ exhibited a 74 meq/100 g of CEC. Comparatively, synthesized NaA-zeolite was made from the reaction between metakaolin and NaOH. This NaA-zeolite showed much higher CEC of 236 meq/100 g, two times higher than natural zeolite.

Distribution ratio K_d can well reflect the selective uptake of synthesized minerals for Sr and Cs ions. Similar to CEC, it is also controlled by their isomorphous substitutions of different valent ions and poor crystallization. Table 5 shows the results of distribution ratios K_d of these synthesized minerals. Synthesized NaA-zeolite had an excellent selective uptake for both Cs and Sr ions. The distribution ratios K_d were 13 758 ml/g for Cs ion and 82 271 ml/g for Sr ion, respectively, 2.1–4.5 times higher than those of natural zeolite XJZ. Evidently, poor crystallization of synthesized NaA-zeolite should be responsible for this. (Al + Na)-substituted CSH also gave much stronger selective adsorption. Its distribution ratios K_d increased with the amounts of aluminium-substitution for silicon in the structure of CSH. The distribution ratios K_d of sample A10 were 5843 ml/g for Sr ion and 3724 ml/g for Cs ion, 47–84% larger than CSH without any substitution. This high selectivity probably arises from the amount of aluminium-substitution for silicon and the resulting changes in the structure of CSH as well as a change in the interlayer ions [1].

In practical immobilizing matrix of M-AAS, the formed (Na + Al)-substituted CSH and self-generated zeolitic precursor displayed much poorer crystallization in addition to isomorphous substitution. Therefore, it was the reason why new M-AAS matrix exhibited better immobilizing effect on Sr and Cs ions.

Table 5
Cation exchange capacities and distribution ratio K_d for different minerals

Samples	Proportions (molar ratio)	Sources	Phases	CEC (meq/100 g)	K_d (ml/g)	
					Cs	Sr
A00	CaO/SiO ₂ = 0.8	CaO, amorphous SiO ₂	CSH	32.5	2019	3974
A05	CaO/(SiO ₂ + Al ₂ O ₃) = 0.8, Al ₂ O ₃ /(SiO ₂ + Al ₂ O ₃) = 0.05, Na ₂ O/Al ₂ O ₃ = 0.5	CaO, MK, amorphous SiO ₂ , NaOH	(Na + Al)-CSH	111.8	2245	4779
A10	CaO/(SiO ₂ + Al ₂ O ₃) = 0.8, Al ₂ O ₃ /(SiO ₂ + Al ₂ O ₃) = 0.10, Na ₂ O/Al ₂ O ₃ = 0.5	CaO, MK, amorphous SiO ₂ , NaOH	(Na + Al)-CSH	162.7	3724	5843
Z4A	Na ₂ O/SiO ₂ = 1, Al ₂ O ₃ /SiO ₂ = 2	MK, NaOH	NaA-zeolite	236.4	13758	82271
XJZ		Natural mineral	Clinoptilolite, modernite	74.4	4357	14718

Note: MK: metakaolin; Z4A: synthesized NaA-zeolite.

4. Conclusions

1. Addition of metakaolin provided AAS matrix with excellent Sr and Cs selective adsorption. Compared to the OPC matrix and AAS matrix, the M-AAS matrix exhibited the highest distribution ratio K_d and lowest leaching rate on both Sr and Cs ions.
2. Addition of metakaolin favors the formation of (Al + Na)-substituted CSH and self-generated zeolitic precursor in the AAS matrix. These hydration products exhibited better selective adsorption and CEC for Sr and Cs ions.

References

- [1] S. Komarneni, D.M. Roy, *Science* 221 (1983) 647.
- [2] H.D. Megaw, C. Kelsey, *Nature* 177 (1956) 390.
- [3] S. Komarneni, D.M. Roy, R. Roy, *Cement Concrete Res.* 12 (1982) 773.
- [4] O.P. Shrivastava, F.P. Glasser, *J. Mater. Sci.* 4 (1985) 1122.
- [5] R.W. Crawford, C. McCulloch, M. Anqus, F.P. Glass, A.A. Rahman, *Cement Concrete Res.* 14 (1984) 595.
- [6] H. Fryda, P. Boch, K. Scrivener, in: K.L. Scrivener, J.F. Yong (Eds.), *Mechanisms of Chemical Degradation of Cement-based Systems*, E&FN spon, London, 1997, p. 367.
- [7] S. Bagosi, L.J. Csetenyi, *Cement Concrete Res.* 29 (1999) 479.
- [8] T. Nishi, M. Matsuda, K. Chirro, M. Kikuchi, *Cement Concrete Res.* 22 (1992) 387.
- [9] X.Q. Wu, S. Yen, X.D. Shen, M.S. Tang, *Cement Concrete Res.* 21 (1991) 16.
- [10] C. Shi, X.Q. Wu, M.S. Tang, *Cement Concrete Res.* 19 (1994) 97.
- [11] S.D. Wang, K.L. Scrivener, *Cement Concrete Res.* 25 (1995) 561.
- [12] I.G. Richardson, A.R. Brough, G.W. Groves, C.M. Dobsen, *Cement Concrete Res.* 24 (1994) 813.
- [13] V.D. Glukhovskiy, *Soil Silicates*, Gosstro Publishers, Kiev, Ukraine, 1959.
- [14] O.P. Shrivastava, S. Komarneni, *Cement Concrete Res.* 24 (1994) 573.
- [15] S. Komarneni, D.M. Roy, *J. Mater. Sci.* 20 (1985) 2930.
- [16] K. Saki, M.S. Sayed, N. Hafez, *Cement Concrete Res.* 27 (1997) 1919.
- [17] A. Palomo, M.T. Blanco-Varela, M.L. Granizo, F. Puertas, T. Vazquez, M.W. Grutzeck, *Cement Concrete Res.* 29 (1999) 997.
- [18] A. Palomo, F.P. Glasser, *Br. Ceram. Trans. J.* 91 (1992) 107.
- [19] S.D. Wang, *Adv. Cement Res.* 12 (2000) 163.
- [20] P.I.A. Malek, D.M. Roy, in: *Proceedings of the 10th International Congress on the Chemistry of Cement*, Goteborg, 1997, p. 1024.
- [21] D.M. Roy, *Cement Concrete Res.* 29 (1999) 249.
- [22] S. Diamond, J.J. White, W.L. Dolch, *Am. Mineral.* 51 (1966) 388.
- [23] D.S. Klimesch, A. Ray, *Thermochim. Acta* 30 (1997) 167.
- [24] T. Mitsuda, S. Kobayakawa, H. Toraya, in: *Proceedings of the 8th International Congress on Chemistry of Cements*, Brazil, 1986, p. 173.
- [25] A. Paklomo, M.W. Grutzeck, M.T. Blanco, *Cement Concrete Res.* 29 (1999) 1323.
- [26] F.P. Glasser, *Br. Ceram. Tran. J.* 89 (1990) 195.
- [27] F.C. Yi, G.R. Qian, Y.X. Li, *J. Southwest Univ. Sci. Tech.* 15 (1999) 16 (in Chinese).
- [28] R.E. Grim, in: R.R. Shrock (Ed.), *Clay Mineralogy*, McGraw-Hill, New York, 1953.